# A Multiscale Time-Splitting Discrete Fracture Model of Nanoparticles Transport in Fractured Porous Media

SPE-KSA-110-MS

Society of Petroleum Engineers

# A Multiscale Time-Splitting Discrete Fracture Model of Nanoparticles Transport in Fractured Porous Media

Mohamed F. El-Amin, SPE, Effat University, KSA; Jisheng Kou, Hubei University, China; Shuyu Sun, SPE, KAUST, KSA



This paper was prepared for presentation at the SPE Kingdom of Saudi Arabia Annual Technical Symposium and Exhibition held in Dammam, Saudi Arabia, 24–27 April 2017.



## Abstract

Recently, applications of nanoparticles have been considered in many branches of petroleum engineering, especially, enhanced oil recovery. The current paper is devoted to investigate the problem of nanoparticles transport in fractured porous media, numerically. We employed the discrete-fracture model (DFM) to represent the flow and transport in the fractured formations. The system of the governing equations consists of the mass conservation law, Darcy's law, nanoparticles concentration in water, deposited nanoparticles concentration on the pore-wall, and entrapped nanoparticles concentration in the pore-throat. The variation of porosity and permeability due to the nanoparticles deposition/entrapment on/in the pores is also considered. We employ the multiscale time-splitting strategy to control different time-step sizes for different physics, such as pressure and concentration. The cell-centered finite difference (CCFD) method is used for the spatial discretization. Numerical examples are provided to demonstrate the efficiency of the proposed multiscale time splitting approach.

## Introduction

Nanoparticles have many applications in oil and gas exploration and production. For instance, some kinds of nanoparticles may be used as tracers for exploration of oil and gas and some others can be used in oilfields. When nanoparticles are absorbed on porous walls, the wettability of the reservoir rocks can be changed into the desired one. One kind of polysilicon nanopowder with the range of 10 - 500 nm was used in oilfields to enhance water injection by changing wettability of the porous medium [1]. Ju et al. [1] conducted experiments and introduced a mathematical model for the nanoparticles transport in porous media. Their mathematical model has been suggested based on the model of the particle migration through porous media [2]. El-Amin et al. [3-7] developed some models of transport of nanoparticles in a two-phase flow in porous media. The problem of nanoparticles transport in anisotropic porous media using the multipoint flux approximation was investigated by Salama et al. [8] . Chen et al. [9] introduced a numerical simulation of drag reduction effects by hydrophobic nanoparticles adsorption method in water flooding processes. Chen et al. [10] introduced the dynamic update of anisotropic permeability field during the transport of nanoparticles in the subsurface.

The fractured geological formations are composed into matrix blocks and fractures. The fractures have much higher permeability than matrix blocks, however, they contain a very small volume of fluid compare to matrix blocks. In order to treat the large discrepancy in scales of fractures and matrix blocks, dual-continua and discrete-fracture models have been employed in this type of modeling [12 - 24]. Warren and Root [24] have developed an idealized model to study the behavior flow in fractured porous

media based on dual continua models. Dual-Porosity model was used when two porosity values existed in the domain. The dual-continua models, such as dual-porosity/dual-permeability model [13, 17, 19, 22, 24] treat matrix and fractures as two separated domains, that are theoretically in- terconnected by fluid mass transfer across their interfaces. In the discrete-fracture-model (DFM) [13,16,20,21,27], fractures dimension is taken *n*-1 when the matrix dimension is n.

In this work, a DFM multiscale time-stepping strategy is introduced for the problem of nanoparticles transport in fractured porous media. A semi-implicit scheme is used for the time discretization, while, the cell-centered finite difference (CCFD) technique is used for the spatial discretization. A large time-step size is used for matrix blocks, while a smaller one is used for fractures. The time-step of fractures pressure is partitioned into subtime-steps. Then, we employ a similar time-splitting strategy for concentration equations. Furthermore, we select numerical example to illustrate the efficiency of the current scheme.

## Mathematical Formulation

**Governing equations:** This paper considers the problem of nanoparticles transport with an immiscible incompressible flow in porous media, the system of governing equations consists of continuity, momentum, nanoparticles concentration, deposited nanoparticles con- centration on the pore-wall, and entrapped nanoparticles concentration in the pore-throat. In addition to the variation of porosity and permeability due to the nanoparticles adhering. The governing equations are, [3-6, 8, 10, 11],

***Momentum Conservation (Darcy's Law):***

$$\mathbf{u} = -\mathbf{K}\nabla P \tag{1}$$

where **K** is the permeability tensor $\boldsymbol{K} = \frac{k}{\mu}\boldsymbol{I}$, **I** is the identity matrix and *k* is a positive real number. **u**, *P*, $\mu$, *k* are, respectively, velocity, pressure, viscosity and permeability.

***Mass Conservation:***

$$\boldsymbol{\nabla} \cdot \mathbf{u} = q \tag{2}$$

where $q$ is the external mass flow rate.

***Nanoparticles Transport:*** Assuming that nanoparticles have only one size interval, the transport equation of the nanoparticles in porous media is given as. media is given as [1-6, 8, 10, 11, 25],

$$\phi \frac{\partial C}{\partial t} + \nabla \cdot (\mathbf{u}C - \phi D \nabla C) = R + Q_c \tag{3}$$

where $C$ is the nanoparticles concentrations. $\varphi$ is the porosity. $D$ is the Brownian diffusion. $Q_C$ is the rate of change of particle volume belonging to a source/sink term. $R$ is the net rate of loss of nanoparticles which is defined by,

$$R = \frac{\partial C_{s1}}{\partial t} + \frac{\partial C_{s2}}{\partial t} \tag{4}$$

***Nanoparticles Surface Deposition:*** The surface depositionis expressed by,

$$\frac{\partial C_{s1}}{\partial t} = \begin{cases} \gamma_d |\mathbf{u}| C, & \mathbf{u} \le u_r \\ \gamma_d |\mathbf{u}| C - \gamma_e |\mathbf{u} - u_r| C_{s1}, & \mathbf{u} > u_r \end{cases} \quad (5)$$

where $C_{S1}$ is the deposited nanoparticles concentration on the pore surfaces of the porous medium. $\gamma_d$ is the rate coefficients for surface retention of the nanoparticles. $\gamma_e$ is the rate coefficients for entrainment of the nanoparticles. $u_r$ is the critical velocity of the water phase.

***Nanoparticles Throat Entrapment:*** The rate of entrapment of the nanoparticlesis,

$$\frac{\partial C_{s2}}{\partial t} = \gamma_{pt} |\mathbf{u}| C \quad (6)$$

where $C_{s2}$ is the entrapped nanoparticles concentration in pore throats and $\gamma_{pt}$ is the pore throat blocking constants.

**Porosity and Permeability Variations:** Solid properties such as porosity and permeability may be changed due to nanoparticles pre- cipitation on the walls and throats of the pores. Therefore, it is worth to investigate them. The porosity variation may be defined as,

$$\phi = \phi_0 - \delta\phi \quad (7)$$

where $\varphi_0$ is the initial porosity and,

$$\delta\phi = C_{S1} + C_{S2}, \quad (8)$$

On the other hand, the change in permeability due to nanoparticles deposition on the pore–walls and entrapped in the pore–throats, is represented as [1],

$$\mathbf{K} = \mathbf{K}_0 \left[ (1-f) k_f + f \frac{\phi}{\phi_0} \right]^l \quad (9)$$

$$f = 1 - \gamma_f C_{s2} \quad (10)$$

where $\mathbf{K}_0$ is the initial permeability, $k_f$ is constant for fluid seepage, $\gamma_f$ is the coefficient of flow efficiency for the particles and $2.5 \le l \le 3.5$ is constant.

**Initial and Boundary Conditions:** Consider the computational domain $\Omega$ with the boundary $\partial\Omega$ which is subjected to Dirichlet $\Gamma_D$ and Neumann $\Gamma_N$ boundaries, where $\partial\Omega = \Gamma_D \cup \Gamma_N$ and $\Gamma_D \cap \Gamma_N = \emptyset$. At the beginning of the injection process, we have,

$$C = C_{s1} = C_{s2} = 0 \quad \text{in} \quad \Omega \qquad \text{at} \quad t = 0, \quad (11)$$

The boundary conditions are given as,

$$P = P^D \qquad \text{on} \qquad \Gamma_D, \quad (12)$$

$$\mathbf{u} \cdot \mathrm{n} = \mathrm{q}^{\mathrm{N}}, \quad C = C_0, C_{S1} = C_{S2} = 0 \quad \text{on} \quad \Gamma_N. \quad (13)$$

where **n** is the outward unit normal vector to $\partial\Omega$, $P^D$ is the pressure on $\Gamma_D$ and $q^N$ the imposed inflow rate on $\Gamma_N$ , respectively.

**Discrete Fracture Model:** In order to represent the fractures explicitly in fractured porous media, we use the discrete-fracture model (DFM) [16,27]. In the DFM, fracture gridcells are simplified as matrix gridcell interfaces and fractures are surrounded by matrix blocks. Thus, if matrix gridcells are of *n*-dimension, then, fracture gridcells are of (*n*-1)-dimension. The domain is decomposed into the matrix domain, $\Omega_{\mathrm{m}}$ and fracture domain, $\Omega_f$. The pressure equation in the matrix domain is given by,

$$-\nabla \cdot \mathbf{K}_{\mathrm{m}} \nabla P_{\mathrm{m}} = q_m, \tag{14}$$

Assuming that the pressure along the fracture width are constants, and by integration, the pressure equation in the fracture becomes,

$$-\nabla \cdot \mathbf{K}_{\mathrm{f}} \nabla P_{\mathrm{f}} = q_{\mathrm{f}} + Q_{\mathrm{f}}, \tag{15}$$

The matrix-fracture interface condition is given by,

$$P_{\mathrm{m}} = P_{\mathrm{f}} \quad \text{on} \quad \partial\Omega_{\mathrm{m}} \cap \partial\Omega_{\mathrm{f}} \tag{16}$$

where the subscript m represents the matrix domain, while the subscript f represents the fracture domain. $Q_{\mathrm{f}}$ is the mass transfer across the matrix-fracture interface. The nanoparticles transport equation in the matrix domain may be expressed as,

$$\phi_{\mathrm{m}} \frac{\partial C_{\mathrm{m}}}{\partial t} + \nabla \cdot (\mathbf{u}_{\mathbf{m}} C_{\mathrm{m}} - \phi_{\mathrm{m}} D \nabla C_{\mathrm{m}}) = R_{\mathrm{m}} + Q_{c,\mathrm{m}} \tag{17}$$

where $C_{\mathrm{m}}$ is the nanoparticles concentrations in the matrix domain. $Q_{C,\mathrm{m}}$ is the rate of change of particle volume belonging to a source/sink term in the matrix domain. $R_{\mathrm{m}}$ is the net rate of loss of nanoparticles in the matrix domain. On the other hand, the nanoparticles transport equation in fractures is represented by,

$$\phi_{\mathrm{f}} \frac{\partial C_{\mathrm{f}}}{\partial t} + \nabla \cdot (\mathbf{u}_{\mathrm{f}} C_{\mathrm{f}} - \phi_{\mathrm{f}} D \nabla C_{\mathrm{f}}) = R_{\mathrm{f}} + Q_{c,\mathrm{m,f}} \tag{18}$$

where $C_{\mathrm{f}}$ is the nanoparticles concentrations in the fracture domain. $Q_{C,\mathrm{f}}$ is the rate of change of particle volume belonging to a source/sink term in the fracture domain. $R_{\mathrm{f}}$ is the net rate of loss of nanoparticles in the fracture domain. $Q_{C,\mathrm{f}}$ represents the rate of change of particle volume across the matrix-fracture interfaces. The interface condition of the nanoparticles concentration is,

$$C_{\mathrm{m}} = C_{\mathrm{f}} \quad \text{on} \quad \partial\Omega_{\mathrm{m}} \cap \partial\Omega_{\mathrm{f}}. \tag{19}$$

The surface deposition in matrix blocks is given by,

$$\frac{\partial C_{s1,\mathrm{m}}}{\partial t} = \begin{cases} \gamma_d |\mathbf{u}_{\mathrm{m}}| C_{\mathrm{m}}, & \mathbf{u}_{\mathrm{m}} \le u_r \\ \gamma_d |\mathbf{u}_{\mathrm{m}}| C_{\mathrm{m}} - \gamma_e |\mathbf{u}_{\mathrm{m}} - u_r| C_{s1,\mathrm{m}}, & \mathbf{u}_{\mathrm{m}} > u_r \end{cases} \tag{20}$$

where $C_{S}1,\mathrm{m}$ is the deposited nanoparticles concentration on the pore surfaces of the matrix domain. Similarly, surface deposition in the fracture domain is represented by,

$$\frac{\partial C_{s1,\mathrm{f}}}{\partial t} = \begin{cases} \gamma_d |\mathbf{u}_\mathrm{f}| C_\mathrm{f}, & \mathbf{u}_\mathrm{f} \le u_r \\ \gamma_d |\mathbf{u}_\mathrm{f}| C_\mathrm{f} - \gamma_e |\mathbf{u}_\mathrm{f} - u_r| C_{s1,\mathrm{f}}, & \mathbf{u}_\mathrm{f} > u_r \end{cases} \tag{21}$$

where $C_{s1,\mathrm{f}}$ is the deposited nanoparticles concentration on the pore surfaces of the fracture domain with the interface condition,

$$C_{\mathrm{s1,m}} = C_{\mathrm{s1,f}} \quad \text{on} \quad \partial\Omega_\mathrm{m} \cap \partial\Omega_\mathrm{f}. \tag{22}$$

Finally, the rate of entrapment of the nanoparticles in the matrix domain is written as,

$$\frac{\partial C_{s2,\mathrm{m}}}{\partial t} = \gamma_{pt} |\mathbf{u}_\mathrm{m}| C_\mathrm{m} \tag{23}$$

where $C_{s2,\mathrm{m}}$ is the entrapped nanoparticles concentration in pore throats of matrix domain. Also, the rate of entrapment of the nanoparticles in the fractures is,

$$\frac{\partial C_{s2,\mathrm{f}}}{\partial t} = \gamma_{pt} |\mathbf{u}_\mathrm{f}| C_\mathrm{f} \tag{24}$$

where $C_{s2,\mathrm{f}}$ is the entrapped nanoparticles concentration in pore throats of fracture with the following interface condition,

$$C_{\mathrm{s2,m}} = C_{\mathrm{s2,f}} \quad \text{on} \quad \partial\Omega_\mathrm{m} \cap \partial\Omega_\mathrm{f}. \tag{25}$$

## Multiscale Time-Splitting and Spatial Discretization

In the multiscale time-splitting method, we employ a different time step-size for each time derivative term as they have different physics. For example, the time-step size for the pressure can be larger than it of the nanoparticles concentration. Also, the fractures pressure may have a larger time-step size than one for the matrix. So, we may use a small time step-size for the pressure in fractures, and so on. We use the CCFD method for the spatial discretization. The CCFD method is locally conservative and equivalent to the quadratic mixed finite element method (see Ref. [26]).

**Multiscale Time-Splitting Approach for Pressure:** Now, let us introduce the time discretization for the pressure in the matrix domain. The total time interval $[0,T]$ is divided into $N_{p,\mathrm{m}}$ steps, i.e., $0 = t^0 < t^1 < \cdots < t^{Np,\mathrm{m}} = T$ and the time step length is $\Delta t^i = t^{i+1} - t^i$. Therefore, we divide each subinterval $(t^i, t^{i+1}]$ into $N_{p,\mathrm{f}}$ sub-subintervals as $(t^i, t^{i+1}] = \cup_{j=0}^{N_{p,\mathrm{f}}-1} \left(t^{i,j} - t^{i,j+1}\right)$, where $t^{i,0} = t^i$ and $t^{i,Np,\mathrm{f}} = t^{i+1}$ and $\Delta t^{i,j} = t^{i+1,j} - t^{i,j}$. In the following, $b$ refers to the boundary of the matrix gridcells $K$ such that its area is $|K|$, and $|b|$ is its length. $\mathbf{n}_b$ is a unit normal vector pointing from $K$ to $K^0$ on each interface $b \in \partial K \cap \partial K^0$. The flux across the boundary $b$ of the gridcell $K$ is denoted by x. $d_{K,b}$ is the distance from the central points of the cell $K$ and the cell boundary $b$. $d_{K,K^0}$ is distance between the central points of the cells $K$ and $K^0$. When $b$ is located on the entire domain boundary, the pressure is provided by Dirichlet boundary conditions, $b \in \Gamma^D$. Otherwise, the Neumann conditions $b \in \partial\Omega^N$ is used to calculate fluxes.

**Multiscale Time-Stepping of the Concentration Equation:** On the other hand, as the nanoparticles concentrations vary more rapidly than the pressures. We also use a smaller time-step size for the concentrations in matrix domain and the smallest time-step size for the concentrations in fractures. The

backward Euler time discretization is used for the equations of concentration and the deposited nanoparticles concentration on the pore–walls and entrapped nanoparticles concentration in the pore-throats. Therefore, the system of governing equations is solved based on the multiscale time-splitting technique. Now, let us divide the time-step $(t^{i,j}, t^{i,j+1}]$ of the fractures pressure into $N_{c,\mathrm{m}}$ sub-steps such that $(t^{i,j}, t^{i,j+1}] = \cup_{j=0}^{N_{c,\mathrm{m}}-1}\left(t^{i,j,k} - t^{i,j,k+1}\right]$, $t^{i,j,0} = t^{i,j}$ and $t^{i,j,N_{s,\mathrm{m}}} = t^{i,j+1}$. This time discretization is employed for the saturation in the matrix domain. Moreover, we use a smaller time-step size for the fracture saturation. Thus, we partition the time-step, $(t^{i,j,k}, t^{i,j,k+1}]$ into $N_{c,\mathrm{f}}$ time sub-steps as $(t^{i,j,k}, t^{i,j,k+1}] = \cup_{j=0}^{N_{c,\mathrm{f}}-1}\left(t^{i,j,k,l} - t^{i,j,k,l+1}\right]$, where $t^{i,j,k,0} = t^{i,j,k}$ and $t^{i,j,k,N_{c,\mathrm{f}}} = t^{i,j,k+1}$.

## Results and Discussion

In order to investigate the efficiency of the numerical scheme and to get physical insight, we present two numerical examples. A domain of dimensions (10 m, 10 m, 1 m) is employed for Examples 1 and 2. The physical and computational parameters are given in Table 1.

**Table 1:** Physical and computational parameters of Examples 1-2.

| Parameter | Example 1 | Example 2 |
|---|---|---|
| Domain dimensions (m) | $10 \times 10 \times 1$ | $10 \times 10 \times 1$ |
| Fracture aperture (m) | 0.01 | 0.01 |
| $\phi_{\mathrm{m}}$ | 0.3 | 0.2 |
| $\phi_{\mathrm{f}}$ | 1 | 1 |
| $K_{\mathrm{m}}$ (md) | 100 | 100 |
| $K_{\mathrm{f}}$ (md) | $10^5$ | $10^4$ |
| $\mu$ (cP) | 1 | 1 |
| $P_{\mathrm{m}}^D$ (bar) | 0.1 | 0.15 |
| $P_{\mathrm{f}}^D$ (bar) | $10^{-4}$ | $10^{-3}$ |
| Injection rate (PVI) | 0.15 | 0.2 |
| Total gridcells | 816 | 816 |
| $\Delta t$ (days) | 0.16 | 0.075 |
| $N_{p,\mathrm{f}}$ | 1 | 2 |
| $N_{c,\mathrm{m}}$ | 1 | 1 |
| $N_{c,\mathrm{f}}$ | 5 | 6 |
| $c_0$ | 0.1 | 0.1 |
| $D(\mathrm{m}^2/s)$ | 5.6e-6 | 5.6e-6 |

In this first example, we simulate the injection of nanoparticles-water suspension with a rate of 0.15 pore volume injection (PVI) until 0.45 pore volume (PV). In the first example, the domain is composed of two perpendicular fractures with different orientation. The nanoparticles concentration in the water is $c_0 = 0.1$ at the well at left-bottom corner of the fractured domain. The permeability in the fractures is $10^5$ md and in the matrix is 100 md. The total number of gridcells of matrix and fractures, is 816. Also, Table 1 shows the outer (matrix pressure) time-step size $\Delta t = 0.16$ and other levels of the multiple sub-timing numbers, namely, $N_{p,\mathrm{f}} = 1$, $N_{c,\mathrm{m}} = 1$ and $N_{c,\mathrm{f}} = 5$. Fig. 1 shows the nanoparticles concentration distribution in the domain. From this figure, we may observe that the nanoparticles move rapidly inside the fractures, then they imbibe into the matrix at the internal side. Moreover, the distribution of the concentration of deposited nanoparticles, $c_{s1}$ is illustrated in Fig. 2. It can be seen from this figure that $c_{s1}$ in fractures is much higher than it in matrix blocks. A similar behavior about $c_{s2}$ can be seen in Fig. 3. Also, the pressure distribution is shown in Fig. 4.

In the second example, we construct a network composed of multiple interconnected fractures in the porous medium. The distribution of the nanoparticles concentration is shown in Fig. 5. Moreover, the distribution of the deposited nanoparticles concentration is presented in Fig. 6, while, the distribution of the entrapped nanoparticles concentration in pore-throats is shown in Fig. 7.

## Summary

In this work, we investigated the transport of nanoparticles in fractured porous media using the DFM multiscale time-stepping method. We employed a semi-implicit time scheme for time discretization, and the CCFD method was used for the spatial discretization. A large time-step size is used for transport in matrix blocks, while a smaller one is used for fractures. The time-step of the pressure in fractures is partitioned into smaller subtime-steps. Similarly, the concentration, deposited concentration, and entrapped concentration have a bigger time-stepping in matrix blocks, while fine ones in fractures. We provided two numerical examples with different configu- rations to show the efficiency of the proposed scheme. The nanoparticles-water suspension transfers rapidly through the fractures. So, exist of fractures in the reservoir may enhance the water distribution and therefore the oil recovery of the fractured medium.

## Acknowledgements

The author is thankful to the Effat University Deanship of Graduate Studies and Researchfor providing the financial support through internal research grants system, Decision No. UC#4/5.JAN.2017/10.1-24d.

## References

[1] Ju, B. and Fan, T. (2009), Experimental study and mathematical model of nanoparticle transport in porous media, Powder Technology, vol.192, pp. 195-202.

[2] Liu, X.H. and Civian, F. (1994), Formation damage and skin factor due to filter cake formation and fines migration in the near–wellbore region, SPE-27364, SPE Symposium on Formation Damage Control, Lafayette, Louisiana.

[3] El-Amin, M.F., Salama, A. and Sun, S. (2012), Modeling and simulation of nanoparticles transport in a two-phase flow in porous media, SPE-154972, SPE International Oilfield Nanotechnology Conference and Exhibition, Noordwijk, The Netherlands.

[4] El-Amin, M.F., Sun, S. and Salama, A. (2012), Modeling and simulation of nanoparticle transport in multiphase flows in porous media: CO2 sequestration, SPE-163089, Mathematical Methods in Fluid Dynamics and Simulation of Giant Oil and Gas Reservoirs.

[5] El-Amin, M.F., Sun, S. and Salama, A. (2013), Enhanced oil recovery by nanoparticles injection: modeling and simulation, SPE-164333, SPE Middle East Oil and Gas Show and Exhibition held in Manama, Bahrain.

[6] El-Amin, M.F., Salama, A. and Sun, S. (2015), Numerical and dimensional analysis of nanoparticles transport with two-phase flow in porous media, J Petrol. Sc. Eng., vol. 128, pp. 53-64.

[7] El-Amin, M. F., Kou, J. and Sun Sun (2017), Convergence analysis of the nonlinear iterative method for two-phase flow in porous media associated with nanoparticle injection, Int. J. Num. Meth. Heat Fluid Flow, Accepted.

[8] Salama, A., Negara, A., El-Amin, M.F. and Sun, S. (2015), Numerical investigation of nanoparticles transport in anisotropic porous media, J. Contaminant Hydrology, vol. 181, pp. 114-130.

[9] Chen, H., Di, Q., Ye, F., Gu, C. and Zhang, J. (2016), Numerical simulation of drag reduction effects by hydrophobic nanoparticles adsorption method in water flooding processes, J. Natural Gas Science and Engineering, vol. 35, pp. 1261-1269.

[10] Chen, M.H., Salama, A. and El-Amin, M.F. (2016), Numerical aspects related to the dynamic update of anisotropic permeability field during the transport of nanoparticles in the subsurface, Procedia Computer Science, vol. 80, pp. 1382-1391.

[11] El-Amin, M.F., Kou, J., Salama, A. and Sun, S., (2016), An iterative implicit scheme for nanoparticles transport with two-Phase flow

in porous media, Procedia Computer Science, vol. 80, pp. 1344-1353.

[12] Baca, R. G. Arnett, R. C. and Langford, D. W. (1984), Modelling fluid flow in fractured-porous rock masses by finite-element techniques, Int. J. Numerical Methods in Fluids, vol. 4, no. 4, pp. 337-348.

[13] Barenblatt, G., Zheltov, Y. and Kochina, I. (1983), Basic concepts in the theory of seepage of homogeneous fluids in fissurized rocks, Journal of Applied Mathematics and Mechanics, vol. 24, no. 5, pp. 1286-1303.

[14] El-Amin, M.F., (2017), Analytical solution of the apparent-permeability gas-transport equation in porous media, The European Physical Journal Plus. 132, pp. 129.

[15] Ghorayeb, K. and Firoozabadi, A., (2000), Numerical study of natural convection and diffusion in fractured porous media, SPE Journal, vol. 5, no. 1, pp. 12-20.

[16] Hoteit, H. and Firoozabadi, A. (2008), An efficient numericalmodel for incompressible two-phase flow in fractured media, Advances in Water Resources, vol. 31, no. 6, pp. 891-905.

[17] Kazemi, H. (1969), Pressure transient analysis of naturally fractured reservoirs with uniform fracture distribution, SPE Journal, vol. 9, no. 4, pp. 451-462.

[18] Kazemi, H., Gilman, J. R. and Elsharkawy, A. M. (1992), Analytical and numerical solution of oil recovery from fractured reservoirs with empirical transfer functions, SPE Reservoir Engineering, vol. 7, no. 2, pp. 219-227.

[19] Kazemi, H. and Merrill, L. S. (1979), Numerical simulation of water imbibition in fractured cores, Old SPE Journal, vol. 19, no. 3, pp. 175-182.

[20] Lee, S. H., Jensen, C. L. and Lough, M. F. (2000), Efficient finite-difference model for flow in a reservoir with multiple length-scale fractures, SPE Journal, vol. 5, no. 3, pp. 268-275.

[21] Noorishad, J. and Mehran, M. (1982), An upstream finite element method for solution of transient transport equation in fractured porous media, Water Resources Research, vol. 18, no. 3, pp. 588-596.

[22] Pruess, K. and Narasimhan, T.N. (1985), A practical method form modeling fluid and heat flow in fractured porous media, SPE Journal, vol. 25, no. 1, pp. 14-26.

[23] Thomas, L. K., Dixon, T. N. and Pierson, R. G. (1983), Fractured reservoir simulation, SPE Journal, vol. 23, no. 1, pp. 42-54.

[24] Warren, J. E. and Root, P.J. (1963), The behavior of naturally fractured reservoirs, Old SPE Journal, vol. 3, no. 3, pp. 245-255.

[25] Gruesbeck, C. and Collins, R.E. (1982), Entrainment and deposition of fines particles in porous media, SPE Journal, vol. 24, pp. 847-856.

[26] Arbogast, T. and Wheeler, M.F. and Yotov, I (1997), Mixed finite elements for elliptic problems with tensor coefficients as cell-centered finite differences, SIAM Journal on Numerical Analysis, vol. 34, no. 2, pp. 828-852.

[27] Kou, J. and Sun, S. and Yu, B. (2011), Multiscale time-splitting strategy for multiscale multiphysics processes of two-phase flow in fractured media, Journal of Applied Mathematics, vol. 2011, Article ID 861905.

# Figures

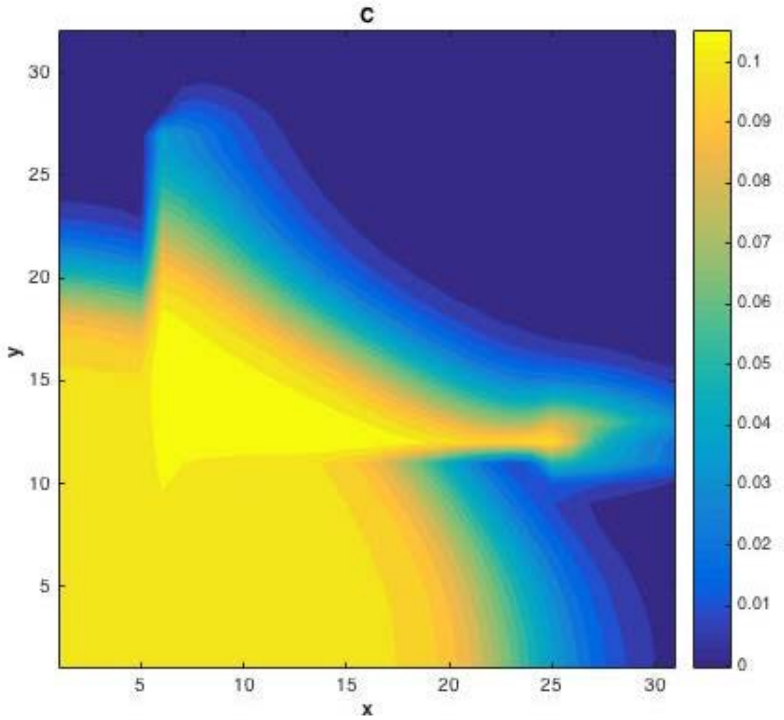


**Fig. 1-** Distribution of nanoparticles concentration at 0.45 PV: Example 1

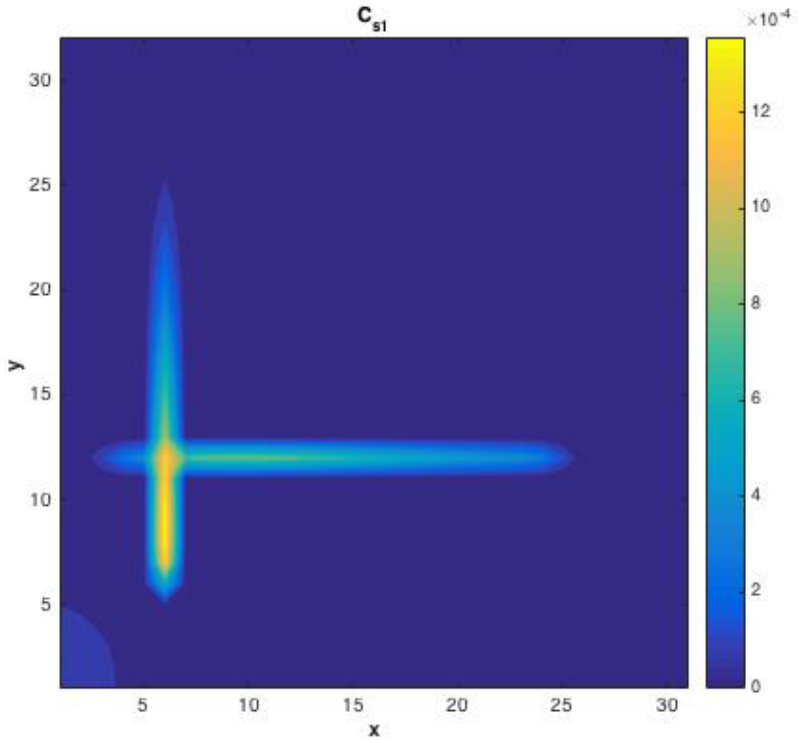


**Fig. 2 -** Distribution of deposited nanoparticles concentration on the pore-wall at 0.45 PV: Example 1

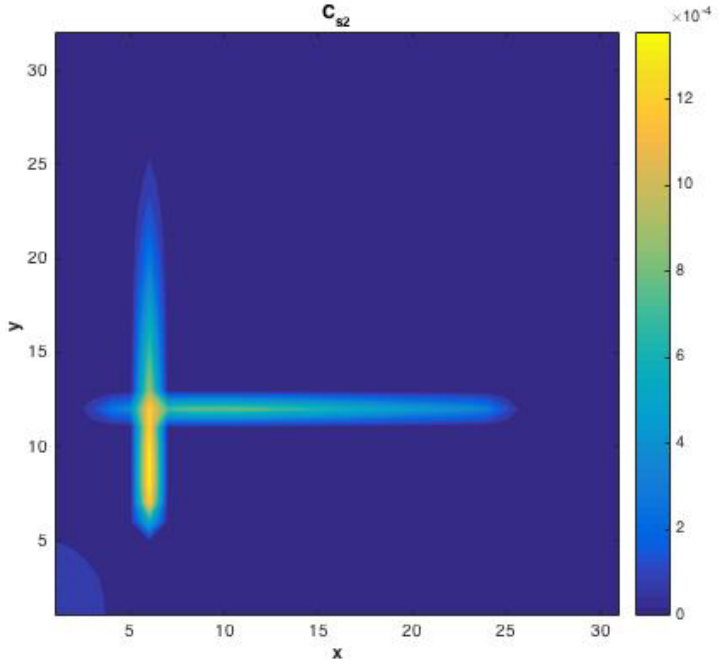


**Fig. 3 -** Distribution of entrapped nanoparticles concentration in the pore-throat at 0.45 PV: Example 1

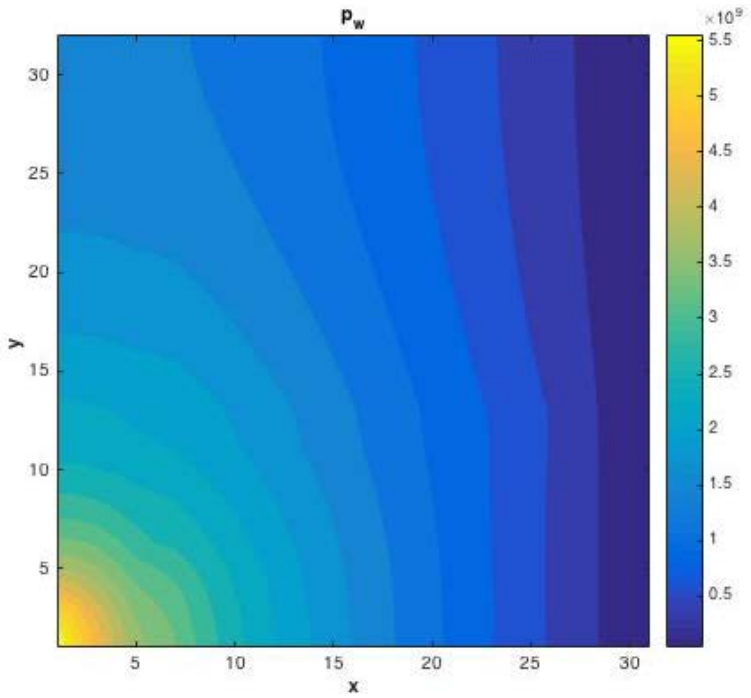


**Fig. 4 -** Distribution of pressure at 0.45 PV: Example 1

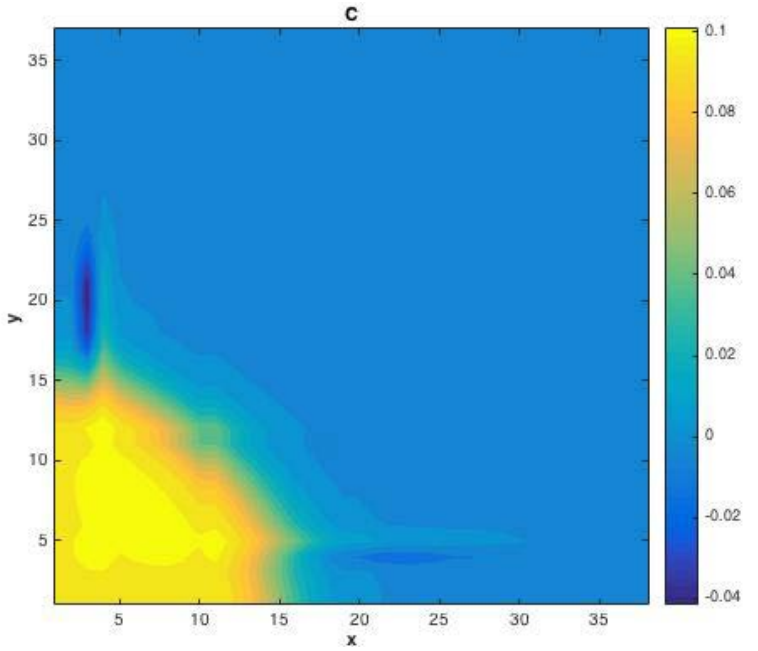


**Fig. 5 -** Distribution of nanoparticles concentration at 0.35 PV: Example 2

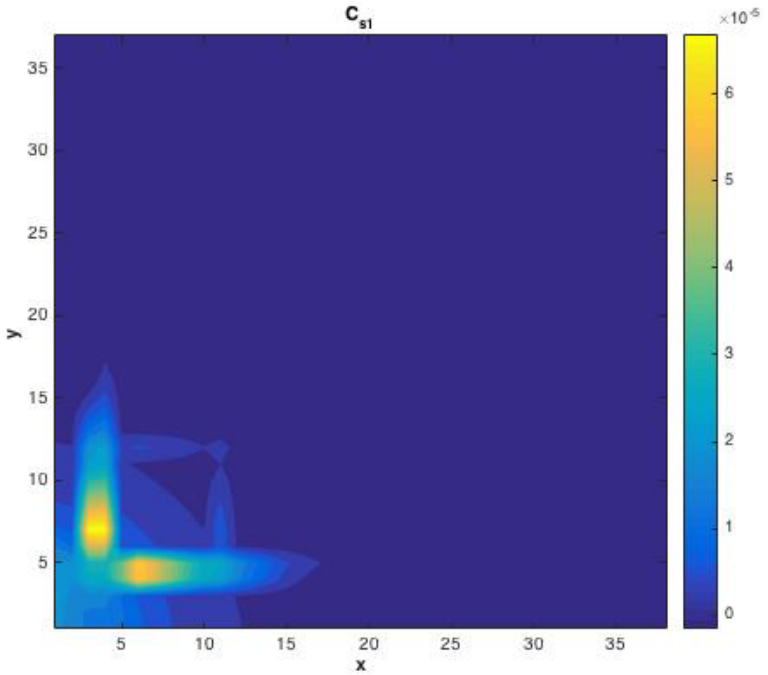


**Fig. 6 -** Distribution of the deposited nanoparticles concentration on pore-walls at 0.35 PV: Example 2

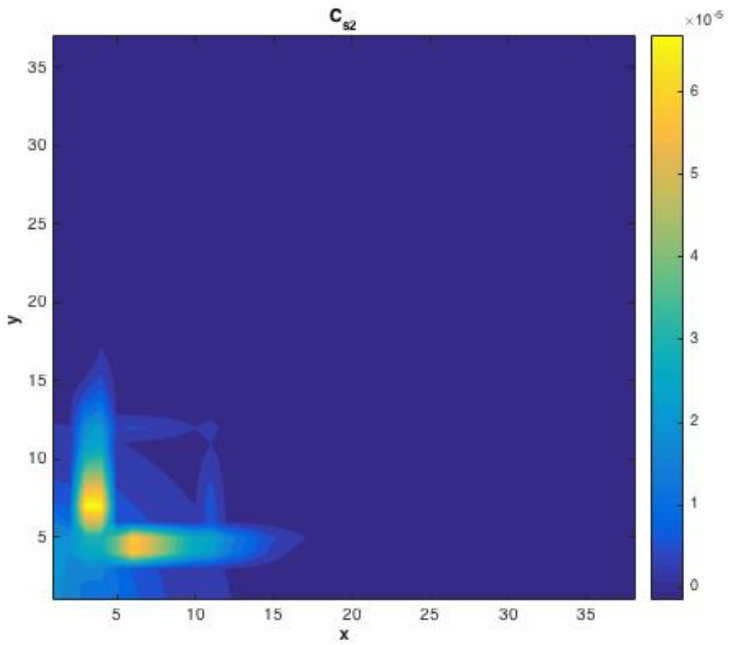


**Fig. 7 -** Distribution of the entrapped nanoparticles concentration in pore-throats at 0.35 PV: Example 2